

## Isotope offsets in marine diatom $\delta^{18}\text{O}$ over the last 200 ka

George E.A. Swann<sup>1\*</sup>, Melanie J. Leng<sup>1,2</sup>, Hilary J. Sloane<sup>1</sup>, Mark A. Maslin<sup>3</sup>

<sup>1</sup>NERC Isotope Geosciences Laboratory, British Geological Survey, Keyworth, Nottingham, NG12 5GG, UK

<sup>2</sup>School of Geography, University of Nottingham, Nottingham, NG7 2RD, UK

<sup>3</sup>Environmental Change Research Centre, Department of Geography, University College London, Pearson Building, Gower Street, London, WC1E 6BT, UK

\* corresponding author [gean@bgs.ac.uk](mailto:gean@bgs.ac.uk)

### Abstract

Previous work has suggested that a species effect may be present in diatom oxygen isotope ratios ( $\delta^{18}\text{O}_{\text{diatom}}$ ). While predominantly attributed to be a size related species effect, currently the precise mechanism remains unknown. Here, two size fractions of diatoms (38-75  $\mu\text{m}$  and  $>100 \mu\text{m}$ ) covering the last 200 ka are analysed for  $\delta^{18}\text{O}$  from ODP Site 882 in the North West Pacific Ocean. Synchronous variations of up to 13‰ occur in both size fractions. However, large isotope offsets (mean = 2.02‰) exist between the two fractions with no relationship between their magnitude and the overlying palaeoenvironmental conditions. In contrast to earlier work from the same site, no one size fraction is constantly higher or lower in  $\delta^{18}\text{O}$  relative to the other. As such, the dominant mechanism is most likely separate to the size effect previously detected. In addition, no relationship exists between the magnitude of the offsets and the species composition of the two size fractions. The presence of these isotope offsets imposes significant constraints upon the future use of  $\delta^{18}\text{O}_{\text{diatom}}$  in palaeoceanographic reconstructions and reiterates the need to extract and analyse only species and size specific diatom samples.

*Keywords:* biogenic silica, disequilibrium effects, vital effects, North Pacific Ocean, opal

### 1. Introduction

Measurements of diatom oxygen isotopes ( $\delta^{18}\text{O}_{\text{diatom}}$ ) are increasingly being used as a means of obtaining palaeoenvironmental and palaeoclimatic records from sedimentary sequences devoid of carbonates (e.g., Shemesh *et al.*, 1994; Morley *et al.*, 2005). The need for such measurements, for example in high latitude regions, is highlighted by the absence of more traditional materials at these locations for obtaining  $\delta^{18}\text{O}$  data, e.g., foraminifera in marine systems and ostracods in lacustrine systems. With high latitude regions particularly sensitive to climate change, so the number of  $\delta^{18}\text{O}_{\text{diatom}}$  measurements is likely to expand as both the procedures and chemicals used for analysing  $\delta^{18}\text{O}_{\text{diatom}}$  become simpler and less hazardous (e.g., Lücke *et al.*, 2005).

An important feature of almost all samples currently analysed for  $\delta^{18}\text{O}_{\text{diatom}}$  is the large number of individual diatom species which may be present within a single sample. In direct contrast to biogenic carbonates, the smaller size of diatom valves (usually c. 5  $\mu\text{m}$  to c. 40  $\mu\text{m}$ ) together with static effects prevents the numerous frustules required for a single isotope measurement from being “picked out” by hand. While in some cases the use of SPLITT (Rings *et al.*, 2004) or sieving at different size fractions (Swann *et al.*, 2006) can result in near or complete mono-species specific samples, in most instances samples analysed for  $\delta^{18}\text{O}_{\text{diatom}}$  are comprised of multiple species, the relative proportions of which may vary considerably throughout a stratigraphical sequence (e.g., Leng *et al.*, 2001). Consequently, records of  $\delta^{18}\text{O}_{\text{diatom}}$  may be complicated by the inclusion of taxa in samples that bloom in different seasons or habitats (Raubitschek *et al.*, 1999; Swann *et al.*, 2006), as well as possible inter and intra-species vital effects.

At present, the occurrence of vital effects in  $\delta^{18}\text{O}_{\text{diatom}}$  is unclear. While vital effects have been widely documented in biogenic carbonates such as foraminifera and ostracods (Duplessy *et al.*, 1970; Wefer and Berger, 1991; Spero and Lea, 1993, 1996; Spero *et al.*, 1997; Xia *et al.*, 1997; Bemis *et al.*, 1998; von Grafenstein *et al.*, 1999; Chivas *et al.*, 2002; Holmes and Chivas, 2002), almost all culture (Binz, 1987; Brandriss *et al.*, 1998; Schmidt *et al.*, 2001), down-core (Juillet-Leclerc and Labeyrie, 1987; Shemesh *et al.*, 1995) and water column studies (Moschen *et al.*, 2005) have found no clear evidence of a vital effect in  $\delta^{18}\text{O}_{\text{diatom}}$ . Recent work, however, has shown the potential for  $\delta^{18}\text{O}_{\text{diatom}}$  vital effects to exist with offsets of up to 3.51‰ (mean offset = 1.23‰,  $n = 25$ ) observed between two size fractions of diatoms at Ocean Drilling Project (ODP) site 882 in the North West Pacific Ocean between 2.84 Ma and 2.57 Ma (Swann *et al.*, 2007). The presence of large  $\delta^{18}\text{O}_{\text{diatom}}$  offsets up to this magnitude creates significant uncertainty over the validity of many existing  $\delta^{18}\text{O}_{\text{diatom}}$  based reconstructions and may limit future measurements of  $\delta^{18}\text{O}_{\text{diatom}}$  to samples dominated by only a single taxa over a small size range. At present, however, the evidence for a vital effect in  $\delta^{18}\text{O}_{\text{diatom}}$  is based only on material from one site over a single time interval. In addition, the mechanisms causing the offsets remains unknown. While evidence within Swann *et al.*, (2007) points towards the existence of at least a size related effect, there is a need for further research to replicate these results and to investigate the existence of similar  $\delta^{18}\text{O}_{\text{diatom}}$  offsets over other time-frames. Here we extend our investigation into the existence of vital effects in  $\delta^{18}\text{O}_{\text{diatom}}$  by analysing material from ODP Site 882 over the last 200 ka BP (Fig. 1). Similar to our previous work, we find large offsets between different species and size fractions of diatoms. This provides further evidence that vital effects may exist within  $\delta^{18}\text{O}_{\text{diatom}}$ .

## 2. Methodology

Sediment samples, each 1 cm thick, were collected from ODP Site 882 in the North West Pacific Ocean (50°22'N, 167°36'E) (Fig. 1). Sample ages in this study were taken from a magnetic susceptibility and GRAPE density derived age model with additional cross correlation between benthic  $\delta^{18}\text{O}_{\text{foram}}$  records from ODP Site 882 and 883 used to verify the stratigraphy (Haug, 1995). Samples for  $\delta^{18}\text{O}_{\text{diatom}}$  were prepared using the three-stage methodology detailed in Swann *et al.*, (2006) which emphasises the need to visually

inspect the diatom flora to identify collectible size fractions which minimise diatom species diversity while generating sufficient material for isotope analysis. In summary, sediment samples covering the last 200 ka (MIS 1-7) were sieved at 38  $\mu\text{m}$ , 75  $\mu\text{m}$  and 100  $\mu\text{m}$  with the 38-75  $\mu\text{m}$  and >100  $\mu\text{m}$  size fractions retained for isotope analysis. While the size range of each fraction would ideally have been reduced to create more sieve bins, e.g., 38-50  $\mu\text{m}$ , 50-75  $\mu\text{m}$  etc, this was not possible due to the necessity of extracting sufficient material for isotope analysis (c. 5 mg). Sieve bins for size fractions smaller than 38  $\mu\text{m}$  were also not suitable for isotope analysis due to the large number of different diatom taxa in this size range and due to the presence of multiple fragments of larger sized diatoms.

Sieved samples were subsequently treated with 30%  $\text{H}_2\text{O}_2$  and 5% HCl to remove organic material and carbonates before being further cleaned of non-diatom contaminants using sodium polytungstate (SPT), a heavy liquid, at a series of specific gravities from 2.10-2.25 g/ml (Morley *et al.*, 2004). The use of SPT was particularly important for the smaller 38-75  $\mu\text{m}$  size fraction where the relative amount of contaminants was significantly higher. In this study, samples were balanced on top of 6 ml of SPT and centrifuged at 2,500 rpm for 20 minutes. This resulted in denser material, such as silts and clays, sinking to the bottom of the centrifuge tube while diatoms remained suspended on top of or in the solution. All samples were centrifuged in SPT at three different specific gravities: firstly at a density of 2.25 g/ml, secondly at a density of 2.20 g/ml and finally at a density of 2.10 g/ml. This SPT procedure was repeated according to need up to three times. Samples still containing significant visible amounts of non-diatom contaminants after this were disregarded for isotope analysis. After the final SPT wash, samples were centrifuge washed three times at x1500 rpm for 5 minutes and then re-sieved at 5  $\mu\text{m}$  using cellulose nitrate membrane filters to remove all traces of the SPT.

Samples of the final purified, but unfluorinated, diatom material were mounted on a coverslip using a Naphrax<sup>®</sup> mounting media and visually checked for contamination under a light microscope. Further SEM analyses were undertaken on selected samples to ensure diatom purity. For the light microscopy work, contamination was assessed following the semi-quantitative approach of Morley *et al.*, (2004) but using 30 rather than 10 quadrants on a 100  $\mu\text{m}$   $\times$  100  $\mu\text{m}$  grid graticule. Quadrants were selected in a semi-random way such that areas representative of the whole coverslip were sampled including the edge where more contamination may be present. Samples containing more than a few percent of non-diatom material were disregarded for isotope analysis.

Diatom biovolumes were calculated following the recommendations of Hillebrand *et al.*, (1999) in which species biovolume coefficients are derived from the median dimensions of at least 25 diatom frustules. For example, biovolumes for the *Coscinodiscus* taxa which dominate the samples in this study were treated as a cylinder:

$$V = \pi \cdot r^2 \cdot h$$

(Eq. 1)

where  $v$  is the volume,  $r$  the radius and  $h$  the height of the diatom frustule. All biovolume coefficients calculated here were based on measurements made by light microscopy across all the analysed samples. It was assumed for all measurements that the relative size of the hydroxyl layer was constant across all taxa. Accordingly, no correction was made to account for the hydroxyl layer which is removed during the pre-fluorination stage (see below). The species specific biovolume coefficients were then applied to diatom abundance counts in the purified material (300 frustules per analysed sample) in order to calculate diatom species biovolume data. Frustule fragments were included within the abundance counts, and hence biovolume data, by making an estimation of their size. Given that all fragments are typically  $>38 \mu\text{m}$ , it proved possible with relative ease to identify and count fragments down to an eighth of a frustule. Whilst measurements of diatom biovolume document the volume rather than the mass or amount of oxygen within the frustules and take no account for pore spaces and other voids/irregularities, the values provide a useful tool for identifying the relative contribution of individual taxa to an isotope measurement.

Diatoms were analysed for oxygen isotopes using a step-wise fluorination method to dissociate the silica and liberate the oxygen (described in Leng and Barker (2006)). In brief, the diatom hydrous layers were stripped during a pre-fluorination outgassing stage in nickel reaction tubes using a  $\text{BrF}_5$  reagent at low temperature before full reaction with an excess of reagent at high temperature. Oxygen was converted to  $\text{CO}_2$  following the methodology of Clayton and Mayeda (1963) with  $\delta^{18}\text{O}_{\text{diatom}}$  measured on an Optima dual inlet mass spectrometer.  $\delta^{18}\text{O}_{\text{diatom}}$  values were converted to the SMOW scale using a within-run laboratory standard ( $\text{BFC}_{\text{mod}}$ ) calibrated against NBS28.

### 3. Results

Light microscope and SEM work shows the analysed frustules to be exceptionally well preserved for fossil diatoms (Fig. 2, 3). Levels of non-diatom contamination in both size fractions were also minimal (Fig. 2, 3, 4a). Diatom biovolumes for the 38-75  $\mu\text{m}$  fraction indicate the  $\delta^{18}\text{O}_{\text{diatom}}$  signal to primarily originate from *Actinocyclus curvatulus* (Janisch in A. Schmidt), *Thalassiosira gravis* (Cleve), *Thalassiosira trifulta* group and multiple fragments of the larger *Coscinodiscus radiatus* (Ehrenb.) (Fig. 4b). The high relative biovolume of *C. radiatus* in a few samples of the 38-75  $\mu\text{m}$  fraction is caused by a large number of *C. radiatus* frustule fragments. This is most likely due to the multiple centrifuging and sieving stages required to clean sediment samples for diatom isotope analysis. With some samples requiring more centrifuging/sieving than other samples, large ( $>100 \mu\text{m}$ ) diatom frustules such as *C. radiatus* are in some samples more likely to be broken and fall through to the smaller 38-75  $\mu\text{m}$  size fraction. While in most cases broken fragments were successfully removed by sieving and collecting material with a 75-100  $\mu\text{m}$  size fraction, as indicated in figure 4b this was not always sufficient to remove all fragments. Despite this, all fragments of *C. radiatus* in the 38-75  $\mu\text{m}$  size fraction show all the fully preserved surface characteristics that can be expected with fossilised diatoms with no visible signs of any process which may alter  $\delta^{18}\text{O}_{\text{diatom}}$ .



Samples in the >100  $\mu\text{m}$  fraction are dominated throughout by *C. radiatus* which is constantly above 66%, and typically above 90%, relative biovolume. Increased relative biovolume of *Coscinodiscus marginatus* (Ehrenb.) to c. 20% occurs in the three oldest samples (Fig. 4b). While the >100  $\mu\text{m}$  fraction may potentially contain a large range of different sized diatom frustules, there are few frustules actually above 200  $\mu\text{m}$  in diameter. Measurements across all >100  $\mu\text{m}$  samples indicate a mean frustule diameter of 144  $\mu\text{m}$  and an upper-quartile diameter of 166  $\mu\text{m}$ .

$\delta^{18}\text{O}_{\text{diatom}}$  measurements from both the 38-75  $\mu\text{m}$  and >100  $\mu\text{m}$  fractions show simultaneous variations of up to 13‰ ( $r = 0.84$ ,  $n = 15$ ) over the analysed interval (Fig. 4c). Direct comparisons, however, show the presence of large and highly variable offsets between the two size fractions with a mean offset of 2.02‰ (offset range = 0.33‰ to 3.07‰) (Fig. 4d, Table 1). Replicate analyses indicate an analytical reproducibility ( $1\sigma$ ) of 0.49‰ in the 38-75  $\mu\text{m}$  fraction and 0.28‰ in the >100  $\mu\text{m}$  fraction and 0.48‰ for BFC<sub>mod</sub>, the NIGL within-run laboratory diatom standard. Of the 15 analysed levels, only one level (9.1 ka BP, offset = 0.33‰) contains an isotope offset less than the combined analytical reproducibility for the two size fractions (Root Mean Squared Error (RMSE)) of 0.56‰ (Fig. 4d, Table 1). In contrast to previous work (Swann *et al.*, 2007), the direction of the offsets varies throughout with no one size fraction constantly higher or lower relative to the other.  $\delta^{18}\text{O}_{\text{diatom}}$  is lower in the >100  $\mu\text{m}$  fraction, relative to the 38-75  $\mu\text{m}$  fraction, at 4.7 ka BP, 80.3 ka BP, 96.8 ka BP and 99.3 ka BP (Fig. 4d, Table 1). For all levels in which  $\delta^{18}\text{O}_{\text{diatom}}$  is higher in the >100  $\mu\text{m}$  fraction relative to the 38-75  $\mu\text{m}$  fraction, the mean offset is 2.18‰ (range = 0.63‰ to 3.07‰,  $n=10$ ). For all levels in which  $\delta^{18}\text{O}_{\text{diatom}}$  is higher in the 38-75  $\mu\text{m}$  fraction, the mean offset is 1.70‰ (range = 0.33‰ to 2.50‰,  $n = 5$ ).

#### 4. Discussion

In the sections below we examine mechanisms which have the potential to cause these offsets. Sections 4.1 and 4.2 investigate the extent to which non-vital effect processes, such as sample contamination and silica maturation, together with temporal variations in diatom blooms and environmental conditions, may be contributing to the offsets. With no evidence that these processes are significant, section 4.3 examines whether evidence of a species/vital effect exists within the data.

##### 4.1. Reliability of the $\delta^{18}\text{O}_{\text{diatom}}$ record

###### *4.1.1. Sample contamination*

The quality and reliability of  $\delta^{18}\text{O}_{\text{diatom}}$  data is often questioned over the potential for measurements to be distorted by non-diatom contamination and diatom valve dissolution/diagenesis. As detailed in section 3, the extracted diatoms analysed here are well preserved (Fig. 2, 3). In addition, visual inspections by light microscopy and SEM show that sample contamination is minimal (Fig. 2, 3, 4a). Although sample purity falls to 93% at 46.6 ka BP and 115.7 ka BP in the 38-75  $\mu\text{m}$  fraction, these two samples still represent a

“clean” sample with purity above the 90% threshold recommended by Morley *et al.*, (2005). In addition, if these two levels are removed from the dataset (offsets in these levels are 1.23‰ and 1.67‰ at 46.6 ka BP and 115.7 ka BP respectively) the mean  $\delta^{18}\text{O}_{\text{diatom}}$  offset across all remaining samples increases to 2.11‰. As such, we can be certain that these “less clean” samples are not causing the offsets.

The possible effect of contamination on the measured  $\delta^{18}\text{O}$  signal can be further examined by mass-balance correcting the isotope composition of each sample (Morley *et al.*, 2005). The measured  $\delta^{18}\text{O}$  of all samples can be assumed to be a linear mixture of the  $\delta^{18}\text{O}$  from diatoms and  $\delta^{18}\text{O}$  from contaminant clay. By knowing the  $\delta^{18}\text{O}$  value of the clay contaminants and by using the sample purity data as an estimate of the contamination within the sample, the  $\delta^{18}\text{O}_{\text{clay}}$  signal can be accounted for to provide a contaminant corrected value of  $\delta^{18}\text{O}_{\text{diatom}}$ :

$$\delta^{18}\text{O}_{\text{corrected}} = \frac{\delta^{18}\text{O}_{\text{measured}} - \frac{\text{Contamination (\%)}}{100} \cdot \delta^{18}\text{O}_{\text{clay}}}{\frac{\text{Diatom purity (\%)}}{100}} \quad (\text{Eq. 2})$$

where  $\delta^{18}\text{O}_{\text{corrected}}$  is  $\delta^{18}\text{O}$  corrected for contamination,  $\delta^{18}\text{O}_{\text{measured}}$  is the original  $\delta^{18}\text{O}$  of the analysed sample and  $\delta^{18}\text{O}_{\text{clay}}$  is the  $\delta^{18}\text{O}$  of the contamination. Values of  $\delta^{18}\text{O}_{\text{clay}}$  are usually significantly lower than that for  $\delta^{18}\text{O}_{\text{diatom}}$ . No  $\delta^{18}\text{O}_{\text{clay}}$  values, however, were measured at ODP Site 882 over the analysed interval due to the difficulty in obtaining a 100% pure clay sample representative of the analysed samples. However, using a range of  $\delta^{18}\text{O}_{\text{clay}}$  values from 0‰ to +20‰ shows that the  $\delta^{18}\text{O}_{\text{diatom}}$  offsets can not be explained by different amounts of clay contamination between the two size fractions, with at least 11 of the 15 analysed levels always containing an isotope offset greater than the RMSE (Fig. 5). Indeed, correcting for contamination in some samples results in an increase, rather than decrease, in the magnitude of the isotope offsets.

#### 4.1.2. Silica maturation

A prominent issue affecting records of  $\delta^{18}\text{O}_{\text{diatom}}$  is the possibility of secondary isotope exchanges during sedimentation (Schmidt *et al.*, 1997, 2001; Brandriss *et al.*, 1998; Moschen *et al.*, 2006). This process of silica maturation has yet to be fully understood but has previously been related to a 2.5‰ increase in  $\delta^{18}\text{O}_{\text{diatom}}$  between living and surface sediment diatoms in Lake Holzmaar, Germany (Moschen *et al.*, 2006) and isotope deviations of up to 10‰ in laboratory experiments (Schmidt *et al.*, 1997, 2001; Brandriss *et al.*, 1998).

An important feature of silica maturation is that it may not always visibly alter the diatom frustule and so can not be assessed through light microscopy or SEM (Moschen *et al.*, 2006). No investigation has yet considered whether inter and/or intra-species variations occur in the magnitude of  $\delta^{18}\text{O}_{\text{diatom}}$  secondary isotope exchange. As such, and as also considered in our previous work (Swann *et al.*, 2007), it is conceivable that

the large  $\delta^{18}\text{O}_{\text{diatom}}$  offsets may reflect inter and/or intra-species variations in silica maturation. It is notable, though, that the direction of the offsets varies throughout the interval with no one size fraction constantly higher or lower relative to the other (Fig. 4d). Given that the species biovolumes of the two size fractions does not vary markedly during these changes from one size fraction being isotopically enriched in  $^{18}\text{O}$  relative to the other (Fig. 4b), it seems unlikely that silica maturation, particularly inter-species variations in silica maturation, are exerting a dominant control on the offsets (Fig. 4d). Although the role of silica maturation can not be conclusively ruled out, based on existing studies and the current absence of evidence for inter and intra-species variations in silica maturation isotope exchange, it is reasonable to assume at this current time that silica maturation does not play a significant role in causing the  $\delta^{18}\text{O}_{\text{diatom}}$  offsets observed here.

## *4.2. Non-species effects*

### *4.2.1. Water column variability*

Contemporary evidence from the North Pacific Ocean shows both *C. radiatus*, which dominates the composition of the  $>100\ \mu\text{m}$  fraction (Fig. 4b), and *C. marginatus*, which comprises up to 25% of the biovolume in the three oldest samples of the  $>100\ \mu\text{m}$  fraction, to have similar temporal fluxes throughout the year with peak fluxes in autumn/early winter months (Takahashi, 1986; Takahashi *et al.*, 1996). This is reinforced by sediment trap data from Station 50N, situated close to ODP Site 882 (Fig. 1, Table 2, Onodera *et al.*, 2005). This contrast with the 38-75  $\mu\text{m}$  fraction which is comprised of multiple species which bloom across different seasons (Fig. 4b). For example, while the aforementioned autumn/winter *C. radiatus* constitutes on average 33% of the sample biovolume in the 38-75  $\mu\text{m}$  fraction, *A. curvatulus*, contributing on average 18% of the sample biovolume, predominantly blooms during the spring months at Station 50N (Table 2; Onodera *et al.*, 2005). In addition *T. gravida*, *T. trifulta* and other less common taxa in the 38-75  $\mu\text{m}$  fraction bloom across a number of different seasons (Table 2; Onodera *et al.*, 2005).

With a number of different species contributing to the biovolumes in the 38-75  $\mu\text{m}$  fraction, the  $\delta^{18}\text{O}_{\text{diatom}}$  offsets may be partially explained by temporal variations in the flux of individual diatom taxa (i.e., a seasonality effect). Sea Surface Temperatures (SST) in the region today are c.  $8^\circ\text{C}$  warmer in late summer/autumn than spring (Locarnini *et al.*, 2006). As such, when using a diatom-temperature coefficient of  $-0.2\text{‰}/^\circ\text{C}$  (Brandriss *et al.*, 1998; Moschen *et al.*, 2005), a 1.6‰ offset would exist if all diatoms frustules in the 38-75  $\mu\text{m}$  fraction bloomed in spring and if all frustules in the  $>100\ \mu\text{m}$  fraction bloomed in summer/autumn. Such calculations though are crude as taxa can not be solely defined as spring or autumn blooming. Determining the extent to which temporal variations may be causing the offsets can be better estimated by considering the relative biovolumes of individual diatom species in each analysed sample in relation to the modern day diatom flux and SST data from the region. Monthly diatom flux records for all taxa are documented in Onodera *et al.*, (2005) from a sediment trap at Station 50N at a depth of 3,260 m (Fig. 1). SST from  $50.5^\circ\text{N}$ ,  $167.5^\circ\text{E}$ , also close to ODP Site 882, are included in Locarnini *et al.*, (2006).

Using a diatom-temperature coefficient of  $-0.2\text{‰}/^{\circ}\text{C}$  we calculate that monthly differences in SST and diatom fluxes would result in a maximum offset of  $0.08\text{‰}$  between the two size fractions (mean =  $0.03\text{‰}$ ), significantly less than the RMSE of  $0.56\text{‰}$ . These seasonality effects have virtually no impact on explaining the  $\delta^{18}\text{O}_{\text{diatom}}$  offsets except at 67.7 ka BP when the adjusted offset decreases to  $0.55\text{‰}$  (Table 3).

Sea Surface Salinity (SSS) in the region today varies by a maximum of 0.36 psu throughout the year (Antonov *et al.*, 2006). At present the SSS: $\delta^{18}\text{O}_{\text{water}}$  and consequently SSS: $\delta^{18}\text{O}_{\text{diatom}}$  relationship for the surface waters of the North West Pacific Ocean are unknown, preventing its inclusion within the above calculations. However, using published mixing lines for the North East Pacific Ocean and Okhotsk Sea (Schmidt *et al.*, 1999; Yamamoto *et al.*, 2001), the maximum annual SSS variability of 0.36 psu is equivalent to an annual  $\delta^{18}\text{O}$  variation in the surface waters of  $0.13\text{--}0.14\text{‰}$ . If the same mixing lines are corrected to account for temporal variations in diatom fluxes, similar to the calculations above, this would lead to a maximum offset of only  $0.01\text{‰}$  between the two size fractions (Table 3).

A significant assumption of all the above calculations is that modern day diatom, SST and SSS data are representative of conditions over the last 200,000 years. Today the North West Pacific Ocean is marked by a strong seasonal SST gradient of c.  $8^{\circ}\text{C}$  (Locarnini *et al.*, 2006), which is driven by the presence of a year round halocline and seasonal thermocline. In the past this large SST gradient could have been significantly reduced in response to a reduction or removal of the halocline. At present it is unclear whether the strength of the halocline was reduced in the past, see section 4.3.2. If it was, expected  $\delta^{18}\text{O}_{\text{diatom}}$  offsets from temporal variations in the surface water would be lower than those predicted above due to the reduced seasonal SST gradient that would exist in a more mixed water column. Any change in SSS in response to variations in the halocline strength would also be approximately constant across all months. As such, possible past changes in the monthly SST and SSS gradients are not capable of explaining the  $\delta^{18}\text{O}_{\text{diatom}}$  offsets.

Further issues not considered within the above calculations included diatom depth habitats together with associated changes in temperature, salinity and  $\delta^{18}\text{O}_{\text{water}}$  at different water depths. Diatoms primarily bloom and fix their structurally bonded oxygen isotope ratios in the -Si-O-Si layer within the photic zone. No information exists on the depth of the photic zone at or immediately around ODP Site 882. Estimates from elsewhere in the North Central and North West Pacific Ocean suggest, however, that the photic zone likely extends down to c. 50 m (Komuro *et al.*, 2005; Katsuki and Takahashi, 2005). In addition, studies in the North Central Pacific Ocean indicate that the majority of diatom taxa live in the upper 50 m of the water column (Katsuki *et al.*, 2003; Katsuki and Takahashi, 2005). Measurements of  $\delta^{18}\text{O}_{\text{water}}$  at  $49^{\circ}12'\text{N}$ ,  $156^{\circ}25'\text{E}$ , the closest site to ODP Site 882 for which water column  $\delta^{18}\text{O}$  measurements exist, indicate minimal variation of  $0.22\text{‰}$  through the water column (Schmidt *et al.*, 1999). The total annual salinity range in the upper 50 m of the water column is also low at 0.45 psu (Antonov *et al.*, 2006) while the temperature gradient between the surface and 50 m is negligible, less than  $1^{\circ}\text{C}$ , through most of the year (Locarnini *et al.*, 2006). Although

a 5-6°C temperature-depth gradient is present from July to September, the impact of this on the  $\delta^{18}\text{O}_{\text{diatom}}$  offsets is likely to be low given the high relative proportion of frustules which will bloom towards the surface where light penetration is higher and where vertical differences in the temperature gradient are reduced (Locarnini *et al.*, 2006). Indeed, the overall vertical temperature gradient is smaller than the annual SST variability of 8°C, which was shown above to only explain a maximum of 0.08‰ of the offsets. While we are unable to properly model the impact of these depth related issues due to the absence of sediment trap data from the region recording diatom fluxes at different depths, it is likely that the impact of any of these factors on the  $\delta^{18}\text{O}_{\text{diatom}}$  offsets is within the limits of analytical reproducibility.

Evidence does exist that *T. trifulta* and *T. gravida* are primarily present at a water depth of c. 100 m to c. 200 m in the North Central Pacific Ocean (Katsuki *et al.*, 2003; Katsuki and Takahashi, 2005). It is unclear, though, to what extent these results are indicative of diatom habitats at ODP Site 882. At worst, if we assume that *T. trifulta* and *T. gravida* both precipitate their frustules at a water depth of 100-200 m at ODP Site 882, re-calculation of the above models to take into account modern temperature and salinity values at these depths suggest that a mean offset of 0.39‰ could exist between the two size fractions when using a diatom-temperature coefficient of  $-0.2\text{‰}/^{\circ}\text{C}$ . Again these expected offsets are within the limits of analytical reproducibility and are not capable of explaining any additional  $\delta^{18}\text{O}_{\text{diatom}}$  offsets (Table 3). In addition, these calculated offsets are almost certainly an overestimate since a proportion of the *T. trifulta* and *T. gravida* frustules will live and bloom within the uppermost sections of the water column alongside other taxa, thereby reducing any potential offset.

All of the above calculations in this section contain significant assumptions with regards to diatom depth-habitats, temporal fluxes and past changes in palaeoenvironmental conditions at ODP Site 882. However, all results suggest that the expected  $\delta^{18}\text{O}_{\text{diatom}}$  offsets between the two size fractions arising from temporal and spatial variations in individual diatom taxa blooms are less than the observed isotope offsets between the two size fractions (Table 3). Indeed, all calculations suggest that the measured  $\delta^{18}\text{O}_{\text{diatom}}$  values should, if anything, be lower in the  $>100\ \mu\text{m}$  fraction relative to the 38-75  $\mu\text{m}$  fraction. This is due to *C. radiatus* and *C. marginatus* in the  $>100\ \mu\text{m}$  fraction primarily blooming in autumn/early winter when SST are relatively warm, compared to taxa within the 38-75  $\mu\text{m}$  fraction which bloom to a greater extent in spring when SST are cooler. Since the majority of the analysed levels (10 out of 15) are marked by higher values in the  $>100\ \mu\text{m}$  fraction (Fig. 4d), this reiterates that some other process must be controlling the direction/magnitude and occurrence of the offsets.

#### 4.2.2. Influx of extraneous taxa

Other processes which may cause the isotope offsets include the influx of diatoms from other locations with a different  $\delta^{18}\text{O}_{\text{water}}$ . In particular *T. gravida*, which contributes between 3% and 8% of the biovolume to all samples in the 38-75  $\mu\text{m}$  fraction, is known at some localities to be a coastal taxa. However, it has been

acknowledged that frustules of *T. gravida* at station 50N in the modern ocean may actually originate from sub-surface, not coastal, waters due to their ability to adapt to nutrient rich conditions during periods of reduced water column stability (Onodera *et al.*, 2005). In addition, as detailed above and shown below in section 4.3.1, no relationship exists between the relative biovolume of *T. gravida* in the analysed samples and the magnitude of the  $\delta^{18}\text{O}_{\text{diatom}}$  offsets. Even if *T. gravida* had originated from coastal waters, it is inconceivable given its low relative biovolume (maximum sample biovolume = 8%) that its presence would be sufficient to cause  $\delta^{18}\text{O}_{\text{diatom}}$  offsets as large as those observed here. Quantification of this, however, is not possible due to the uncertainty over where any “coastal” *T. gravida* would originate from.

#### 4.3. Species effects in $\delta^{18}\text{O}_{\text{diatom}}$

$\delta^{18}\text{O}_{\text{diatom}}$  data in Swann *et al.*, (2007), also from ODP Site 882 but covering the interval from 2.84-2.57 Ma, provided the first clear evidence that a species effect may exist in  $\delta^{18}\text{O}_{\text{diatom}}$  with large offsets of up to 3.51‰ observed between two size fractions of diatoms (75-150  $\mu\text{m}$  and >150  $\mu\text{m}$ ). While these offsets may be better described as an isotope vital effect (i.e., non-equilibrium isotope fractionation) the term “species effect” was used since diatom isotope equilibrium in the palaeo sequence remains unknown.

Above in sections 4.1 and 4.2 the possible impact of sample contamination and spatial/temporal variations in the water column have been shown to not be plausible mechanisms in explaining the  $\delta^{18}\text{O}_{\text{diatom}}$  offsets observed here over the last 200 ka. With the offsets greater than the RMSE in 14 of the 15 analysed levels (Fig. 4d, Table 1), the data may provide further evidence of a possible species/vital effect in  $\delta^{18}\text{O}_{\text{diatom}}$ . Although sediment core top studies together with culture and field experiments are needed to confirm this, in the sections below the  $\delta^{18}\text{O}_{\text{diatom}}$  data is examined for any evidence of a systematic species/vital effect which may be initiating or controlling the observed offsets.

##### 4.3.1. Inter-species effects

In contrast to the offsets observed in Swann *et al.*, (2007) in which  $\delta^{18}\text{O}_{\text{diatom}}$  values in the smaller 75-150  $\mu\text{m}$  fraction were greater than the >150  $\mu\text{m}$  fraction, in the samples analysed here the direction of the offsets varies throughout (Fig. 4d). As such, while a size related species effect may play a role in explaining the offsets observed here, other processes must also be occurring. No relationship is apparent between individual diatom species relative biovolumes and the  $\delta^{18}\text{O}_{\text{diatom}}$  offsets ( $p = 0.84, 0.98, 0.73$  and  $0.20$  and  $R^2 = 0.01, 3.46 \times 10^{-5}, 0.01$  and  $0.15$  for *C. radiatus*, *T. trifulta*, *A. curvatulus* and *T. gravida* respectively). In addition, no significant improvement in this relationship can be obtained through any combination of linear or non-linear regression models. Identifying any inter-species effect, however, may be complicated by the additional presence of a size effect, similar to that found in Swann *et al.*, (2007), which could be acting to obscure any inter-species effect signal. In addition, difficulties in generating accurate diatom biovolume measurements may also be preventing detection of any inter-species effect.

Obtaining accurate diatom biovolume measurements is a prominent issue of discussion (see review in Hillebrand *et al.*, 1999). Although inaccuracies exist due to the problems of accounting for diatom fragments and pore spaces/voids, these errors should not be sufficiently large as to completely remove any evidence of a statistical inter-species relationship. Significant uncertainty does exist, however, over the impact of the pre-fluorination outgassing stage on diatom biovolumes. All biovolumes measurements, whether calculated under light-microscopy or otherwise, are derived from the purified unreacted sample (see Methodology). The pre-fluorination stage of the  $\delta^{18}\text{O}_{\text{diatom}}$  analysis, however, removes the hydroxyl layer of the diatom, which can represent a considerable proportion, up to c. 30-35%, of the total diatom biovolume. Currently, it is assumed that the relative size of the hydroxyl layer is constant between and within individual taxa. Whilst no evidence currently exists to contradict this assumption, any variation in the relative thickness or size of the hydroxyl layer will alter the species biovolume of a given sample and potentially lead to the loss of any inter-species effect signal.

During the fluorination process a fluorination yield is calculated from the amount of oxygen actually converted into  $\text{CO}_2$  relative to the amount of gas that would be expected from the equivalent weight of  $\text{SiO}_2$ . With levels of contamination low in the analysed samples, fluorination yields can be interpreted as the hydroxyl layer, and consequently diatom biovolume, lost during the pre-fluorination stage. Yield values are 64.4% for the 38-75  $\mu\text{m}$  fraction and 69.3% for the >100  $\mu\text{m}$  fraction. While the variability within each size fraction is large at 3.3% and 3.7% ( $1\sigma$ ) for the 38-75  $\mu\text{m}$  and >100  $\mu\text{m}$  fractions respectively, this is of a similar magnitude to the 3.0% reproducibility achieved with  $\text{BFC}_{\text{mod}}$ , the NIGL within-run laboratory diatom standard. A paired Wilcoxon signed rank test, a non-parametric alternative to a Student's t-test for related samples, indicates a significant difference between yield values for the two size fractions with larger relative -Si-O-Si layers in the >100  $\mu\text{m}$  fraction ( $p < 0.001$ ). This raises the possibility that fluorination yields, and hence hydroxyl layer thicknesses, are species dependent. To date no study has investigated the existence of inter and intra-species variations in diatom fluorination yields. However, consideration of hydroxyl layer loss during the pre-fluorination out-gassing stage may be crucial for obtaining the accurate diatom biovolume data needed to further investigate and detect possible inter-species effects in  $\delta^{18}\text{O}_{\text{diatom}}$ . Until then, it remains problematic to further investigate the issue of inter-species effects and their contribution to the isotope offsets.

#### 4.3.2. Nutrient species effect

One further process which may lead to offsets in  $\delta^{18}\text{O}_{\text{diatom}}$  involves changes in surface water nutrient availability, which can have significant impacts on diatom physiology (see reviews in Martin-Jézéquel *et al.*, (2000) and Ragueneau *et al.*, (2000, 2006)). Today the region around ODP Site 882 is marked by a strong halocline at c. 150 m, which significantly limits the supply of nutrients to the photic zone (Tabata, 1975; Gargett, 1991). An absence or reduction in the halocline would alter this allowing upwelling of nutrient rich deep water to the surface. To date, relatively few studies have reconstructed palaeoceanographic conditions

and the presence/absence of the halocline over the last 200 ka. The halocline has been shown to have first developed at 2.73 Ma with suggestions that stratification may have continued uninterrupted from this date (Haug *et al.*, 2005; Swann *et al.*, 2006). Using the Holocene as an analogue to MIS 5e, it is therefore likely that the halocline also prevailed during the last interglacial, although no data currently exist to support or contradict this. The situation, though, is less clear during the last glacial. Most studies argue for an enhanced halocline, based on foraminifera stable isotope (Keigwin *et al.*, 1992), diatom assemblage (Sancetta, 1983), biogenic barium (Jaccard *et al.*, 2005) and nitrogen isotope data (Brunelle *et al.*, 2007). Other evidence, however, based on foraminifera stable isotopes, assemblage counts and Mg/Ca ratios argues for a more mixed water column during the last glacial with the modern halocline becoming re-established at 11.1-9.3 ka BP (Sarnthein *et al.*, 2004; 2006). Regardless of whether a halocline did or did not exist in the past, no link is apparent between sample ages and changes in the magnitude/direction of the  $\delta^{18}\text{O}_{\text{diatom}}$  offsets (Fig. 4d). For example, glacial aged samples (which may or may not have been associated with a reduced halocline) can not be related to larger/smaller offsets or one size fraction having a higher  $\delta^{18}\text{O}_{\text{diatom}}$  relative to the other.

Issues of stratification and associated changes in the supply of nitrate, silicate and phosphate to the photic zone, however, may not be the most important variables with regards to changes in diatom physiology. Today large sections of the North Pacific Ocean are Fe limited with respect to diatom growth (Harrison *et al.*, 1999; Tsuda *et al.*, 2003; Yuan and Zhang, 2006). The impact of increased Fe availability on diatoms is well documented with Fe limitation leading to increases in cell Si:N and Si:C ratios and decreases in diatom growth rates (see Hutchins and Bruland, (1998); Takeda, (1998) and reviews in de Baar *et al.*, (2005) and Ragueneau *et al.*, (2006)). Despite this, the impact of changes in Fe availability on  $\delta^{18}\text{O}_{\text{diatom}}$  has yet to be investigated. Previous work, however, has suggested that  $\delta^{18}\text{O}_{\text{diatom}}$  may be influenced by changes in growth rates with less isotope fractionation occurring in fast-growing diatoms (Schmidt *et al.*, 2001). While changes in diatom growth rates, in response to increased/decreased Fe deposition, would be expected to be constant across both the 38-75  $\mu\text{m}$  and >100  $\mu\text{m}$  fractions, we have previously questioned whether this diatom isotope growth effect may influence larger frustules to a greater extent than smaller frustules (Swann *et al.*, 2007). Fe deposition to the open North Pacific Ocean primarily occurs via aeolian transportation from the Badain Juran desert (Duce and Tindale, 1991; Jickells *et al.*, 2005; Yuan and Zhang, 2006). However, similar to results in Swann *et al.*, (2007), no clear link exists between the magnitude or direction of the  $\delta^{18}\text{O}_{\text{diatom}}$  offsets and changes in aeolian/dust deposition to the North Pacific Ocean (Hovan *et al.*, 1991; Kawahata *et al.*, 2000). Likewise, no link exists between the isotope offsets and changes in the accumulation of aeolian deposits at the Chinese Loess Plateau (Sun and An, 2005). As such, it is unlikely that issues of Fe fertilisation and Fe induced changes in diatom growth rates are a dominant factor in explaining the  $\delta^{18}\text{O}_{\text{diatom}}$  offsets.

#### *4.4. Explaining isotope offsets in $\delta^{18}\text{O}_{\text{diatom}}$*

Above, a number of issues have been examined in an attempt to understand the processes which are controlling the observed  $\delta^{18}\text{O}_{\text{diatom}}$  offsets between the two size fractions. However, we are unable to



conclusively explain the offsets based on the data currently available. Indeed many of the seasonality corrections in Section 4.2 result in an increase, rather than decrease, in the magnitude of the  $\delta^{18}\text{O}_{\text{diatom}}$  offsets (Table 3). The majority of the  $\delta^{18}\text{O}_{\text{diatom}}$  offsets in our previous work were attributed to a size related species effect (Swann *et al.*, 2007). A major difference between those results and the offsets shown here are the frequent changes in the direction of the  $\delta^{18}\text{O}_{\text{diatom}}$  offsets over the last 200 ka (Fig. 4d). In addition, here the majority of the analysed levels contain higher  $\delta^{18}\text{O}_{\text{diatom}}$  values in the larger >100  $\mu\text{m}$  fraction relative to the smaller 38-75  $\mu\text{m}$  fraction. In contrast, results in Swann *et al.*, (2007) are marked by higher isotope values in the smaller 75-150  $\mu\text{m}$  fraction relative to the larger >150  $\mu\text{m}$  fraction. On the one hand, it is possible that the processes contributing to the  $\delta^{18}\text{O}_{\text{diatom}}$  offsets are different over each of the two time intervals. Alternatively it is plausible that the mechanisms behind the offsets are the same over both intervals, but that the relative importance of each mechanism has changed. Such a scenario, one of multiple processes in which the relative importance of each can vary with changes in surface water palaeoenvironmental conditions and nutrient availability, would be particularly well suited for explaining the large changes in the direction and magnitude of the  $\delta^{18}\text{O}_{\text{diatom}}$  offsets over the last 200 ka (Fig. 4d).

At present, we are unable to conclude further as to what the potential process or processes controlling the isotope offsets may be. As such, it is feasible that the  $\delta^{18}\text{O}_{\text{diatom}}$  offset are controlled by a combination of inter-species, intra-species, size and nutrient related species effects in addition to possible inter and intra-species variations in diatom secondary isotope exchange. While it seems likely that a species/vital effect is present in  $\delta^{18}\text{O}_{\text{diatom}}$ , further investigation here is hampered by the problems in deriving accurate species biovolume data and by a lack of detailed contemporary information on the systematics of oxygen isotope fractionation and uptake by diatoms. Furthermore, the operation of multiple processes may be blurring evidence for their existence, particularly if the relative importance of any single process can vary over time. Clearly though, the presence of large  $\delta^{18}\text{O}_{\text{diatom}}$  offsets between different samples has significant implications for the future use of  $\delta^{18}\text{O}_{\text{diatom}}$  in palaeoceanographic reconstructions, requiring that future samples be dominated by only a single taxa over a finite size range.

## 5. Conclusion

The presence of large and highly variable isotope offsets in  $\delta^{18}\text{O}_{\text{diatom}}$  at ODP Site 882 over both the samples analysed here (last 200 ka BP) and that in Swann *et al.*, (2007) (2.84 Ma to 2.57 Ma) provides clear evidence that some form of species/vital effect may exist within measurements of  $\delta^{18}\text{O}_{\text{diatom}}$ . Despite this, no clear mechanism or process can be identified to explain these offsets. As such, while measurements of  $\delta^{18}\text{O}_{\text{diatom}}$  remain suitable for providing qualitative palaeoenvironmental information when the magnitude of change is greater than any of the offsets observed here and in our earlier work (current maximum is 3.51‰), significant uncertainty remains over the validity of any quantitative based reconstruction. In order to better constrain these isotope offsets, in-field studies and laboratory culture experiments are needed. In the interim it is essential that increased attention is paid to the species and size composition of diatom samples analysed

for  $\delta^{18}\text{O}_{\text{diatom}}$ . To this end, only species or near-species specific samples that cover a limited size range should be used for diatom isotope analysis. This should apply not only to marine but also to freshwater environments where measurements of  $\delta^{18}\text{O}_{\text{diatom}}$  are increasingly being used in carbonate free systems (see review in Leng and Barker (2006)).

### Acknowledgements

The authors would like to thank Jonaotaro Onodera and Kozo Takahashi for their insightful discussions on diatom fluxes at station 50N and for providing the data in Table 2. Additional thanks are owed to the Ocean Drilling Program (ODP) for making available the sample material and two anonymous reviewers whose comments helped improve the manuscript. This study was carried out during a NERC PhD studentship award (NER/S/A/2004/12193) at UCL and CASE studentship award at NIGL (IP/812/0504) to GEAS.

### References

- Antonov JJ, Locarnini RA, Boyer TP, Mishonov AV, Garcia HE. 2006. World Ocean Atlas 2005. Volume 2: Salinity. S. Levitus, Ed. NOAA Atlas NESDIS 62, U.S. Government Printing Office, Washington, D.C., 182 pp.
- Bemis BE, Spero H, Bijma J, Lea DW. 1998. Reevaluation of the oxygen isotopic composition of planktonic foraminifera: experimental results and revised paleotemperature equations. *Paleoceanography* **13**: 150-160.
- Binz P. 1987. Oxygen-isotope analysis on recent and fossil diatoms from Lake Walen and Lake Zurich (Switzerland) and its application on paleoclimatic studies, PhD Thesis, Swiss Federal Institute of Technology, Zurich, pp. 165.
- Brandriss ME, O'Neil JR, Edlund MB, Stoermer EF. 1998. Oxygen isotope fractionation between diatomaceous silica and water. *Geochim. Cosmochim. Ac.* **62**: 1119-1125.
- Brunelle BG, Sigman DM, Cook MS, Keigwin LD, Haug GH, Plessen B, Schettler G, Jaccard SL. 2007. Evidence from diatom-bound nitrogen isotopes for subarctic Pacific stratification during the last ice age and a link to North Pacific denitrification changes. *Paleoceanography* **22**: PA1215, doi:10.1029/2005PA001205.
- Chivas AR, De Deckker P, Wang SX, Cali JA. 2002. Oxygen-isotope systematics of the nektonic ostracod *Australocypris robusta*. In *The ostracoda: applications in Quaternary Research*, Holmes JA, Chivas AR. (eds). AGU Geophysical Monograph 11, American Geophysical Union: Washington DC; 301-313.
- Clayton RN, and Mayeda TK. 1963. The use of bromine pentafluoride in the extraction of oxygen from oxide and silicates for isotope analysis. *Geochim. Cosmochim. Ac.* **27**: 43-52.
- de Baar HJW, Boyd PW, Coale KH, Landry MR, Tsuda A, Assmy P, Bakker DCE, Bozec Y, Barber RT, Brzezinski MA, Buesseler KO, Boye M, Croot PL, Gervais F, Gorbunov MY, Harrison PJ, Hiscock WT, Laan P, Lancelot C, Law CS, Lavoie M, Marchetti A, Millero FJ, Nishioka J, Nojiri Y, van Oijen T, Riebesell U, Rijkenberg MJA, Saito H, Takeda S, Timmermans KR, Veldhuis MJW, Waite AM, and Wong CS. 2005. Synthesis of iron fertilisation experiments: from the Iron Age in the age of enlightenment. *Journal of Geophysical Research* **110**: C09S16, doi:10.1029/2004JC002601.
- Duce RA, Tindale NW. 1991. Atmospheric transport of iron and its deposition in the ocean. *Limnology and Oceanography* **36**: 1715-1726.
- Duplessy JC, Lalou C, Vinot AC. 1970. Differential isotopic fractionation in benthic foraminifera and paleotemperatures revised. *Science* **213**: 1247-1250.
- Gargett AE. 1991. Physical processes and the maintenance of nutrient-rich euphotic zones. *Limnology and Oceanography* **36**: 1527-1545.
- Harrison PJ, Boyd PW, Varela DE, Takeda S, Shiimoto A, Odate T. 1999. Comparison of factors controlling phytoplankton productivity in the NE and NW subarctic Pacific gyres, *Prog. Oceanogr.* **43**: 205-234.

- Haug GH. 1995. The evolution of Northwest Pacific Ocean over the last 6 Ma: ODP LEG 145. PhD thesis, pp 200., University of Kiel, Kiel, Germany.
- Haug GH, Ganopolski A, Sigman DM, Rosell-Mele A, Swann GEA, Tiedemann R, Jaccard S, Bollmann J, Maslin MA, Leng MJ, Eglinton G. 2005. North Pacific seasonality and the glaciation of North America 2.7 million years ago. *Nature* **433**: 821-825.
- Hillebrand H, Dürselen C-D, Kirschtel D, Pollinger U, Zohary T. 1999. Biovolume calculation for pelagic and benthic microalgae. *J. Phycol.* **35**: 403-424.
- Holmes JA, Chivas AR. 2002. Ostracod shell chemistry – overview. In *The ostracoda: applications in Quaternary Research*, Holmes JA, Chivas AR. (eds). AGU Geophysical Monograph 11, American Geophysical Union: Washington DC; 185-204.
- Hovan SA, Rea DK, Pisias NG. 1991. Late Pleistocene continental climate and oceanic variability recorded in Northwest Pacific sediments. *Paleoceanography* **6**: 349-370.
- Hutchins DA, Bruland KW. 1998. Iron-limited diatom growth and Si:N uptake ratios in a coastal upwelling zone. *Nature* **393**: 561–564.
- Jaccard SL, Haug GH, Sigman DM, Pedersen T., Thierstein HR, Röhl U. 2005. Glacial/interglacial changes in subarctic North Pacific stratification. *Science* **308**: 1003-1006.
- Jickells TD, An ZS, Andersen KK, Baker AR, Bergametti G, Brooks N, Cao JJ, Boyd PW, Duce RA, Hunter KA, Kawahata H, Kubilay N, la Roche J, Liss PS, Mahowald N, Prospero JM, Ridgwell AJ, Tegen I, Torres R. 2005. Global iron connections between desert dust, ocean biogeochemistry, and climate. *Science* **308**: 67-71.
- Juillet-Leclerc A, Labeyrie L. 1987. Temperature dependence of the oxygen isotopic fractionation between diatom silica and water. *Earth Planet. Sc., Lett.* **84**: 69-74.
- Katsuki K, Takahashi K. 2005. Diatoms as paleoenvironmental proxies for seasonal productivity, sea-ice and surface circulation in the Bering Sea during the late Quaternary. *Deep-Sea Res. Pt. II*, **52**: 2110-2130.
- Katsuki K, Takahashi K, Okada M. 2003. Diatom assemblage and productivity changes during the last 340,000 years in the subarctic Pacific. *Journal of Oceanography* **59**: 695-707.
- Kawahata H, Okamoto T, Matsumoto E, Ujiie H. 2000. Fluctuations of eolian flux and ocean productivity in the mid-latitude North Pacific during the last 200 kyr. *Quaternary Science Reviews* **19**: 1279-1292.
- Keigwin LD, Jones GA, Froelich PN. 1992. A 15,000 year paleoenvironmental record from Meiji Seamount, far northwestern Pacific *Earth and Planetary Science Letters* **111**: 425-440.
- Komuro C, Narita H, Imai K, Nojiri Y, Jordan RW. 2005. Microplankton assemblages at Station KNOT in the subarctic western Pacific 1999-2000. *Deep-Sea Research Part II* **52**: 2206-2217.
- Leng MJ, Barker PA, Greenwood P, Roberts N, Reed J. 2001. Oxygen isotope analysis of diatom silica and authigenic calcite from Lake Pinarbasi, Turkey. *Journal of Palaeolimnology* **25**: 343-349.
- Leng MJ, Barker PA. 2006. A review of the oxygen isotope composition of lacustrine diatom silica for palaeoclimate reconstruction. *Earth-Sci. Rev.* **75**: 5-27.
- Locarnini RA, Mishonov AV, Antonov JI, Boyer TP, Garcia HE. 2006. World Ocean Atlas 2005, Volume 1: Temperature. S. Levitus, Ed. NOAA Atlas NESDIS 61, U.S. Government Printing Office, Washington, D.C., 182 pp.
- Lücke A, Moschen R, Schleser GH. 2005. High temperature carbon reduction of silica: A novel approach for oxygen isotope analysis of biogenic opal. *Geochim. Cosmochim. Ac.* **69**: 1423-1433.
- Martin-Jézéquel V, Hildebrand M, Brzezinski MA. 2000. Silicon metabolism in diatoms: implications for growth. *J. Phycol.* **36**: 821-840.
- Morley DW, Leng MJ, Mackay AW, Sloane HJ, Rioual P, Battarbee RW. 2004. Cleaning of lake sediment samples for diatom oxygen isotope analysis. *Journal of Paleolimnology* **31**: 391–401.
- Morley DW, Leng MJ, Mackay AW, Sloane HJ. 2005. Late Glacial and Holocene environmental change in the Lake Baikal region documented by oxygen isotopes from diatom silica. *Global and Planetary Change* **46**: 221-233.
- Moschen R, Lücke A, Schleser G. 2005. Sensitivity of biogenic silica oxygen isotopes to changes in surface water

temperature and palaeoclimatology. *Geophys. Res. Lett.* **32**: L07708, doi:10.1029/2004GL022167.

- Moschen R, Lücke A, Parplies J, Radtke U, Schleser GH. 2006. Transfer and early diagenesis of biogenic silica oxygen isotope signals during settling and sedimentation of diatoms in a temperate freshwater lake (Lake Holzmaar, Germany). *Geochim. Cosmochim. Ac.* **70**: 4367-4379.
- Ragueneau O, Tréguer P, Leynaert A, Anderson RF, Brzezinski MA, DeMaster DJ, Dugdale RC, Dymond J, Fischer G, Francois R, Heinze C, Maier-Reimer E, Martin-Jézéquel V, Nelson DM, Quéguiner B. 2000. A review of the Si cycle in the modern ocean: recent progress and missing gaps in the application of biogenic opal as a paleoproductivity proxy. *Global and Planetary Change* **26**: 317-365.
- Ragueneau O, Schultes S, Bidle K, Claquin P, Moriceau B. 2006. Si and C interactions in the world ocean: Importance of ecological processes and implications for the role of diatoms in the biological pump. *Global Biogeochem. Cycles* **20**: GB4S02 doi:10.1029/2006GB002688.
- Raubitschek S, Lücke A, Schleser GH. 1999. Sedimentation patterns of diatoms in Lake Holzmaar, Germany - (on the transfer of climate signals to biogenic silica oxygen isotope proxies). *Journal of Paleolimnology* **21**: 437-448.
- Rings A, Lücke A, Schleser GH. 2004. A new method for the quantitative separation of diatom frustules from lake sediments. *Limnology and Oceanography Methods* **2**: 25-34.
- Onodera J, Takahashi K, Honda MC. 2005. Pelagic and coastal diatom fluxes and the environmental changes in the northwestern North Pacific during 1997-2000. *Deep-Sea Research Part II* **52**: 2218-2239.
- Sancetta C. 1983. Effect of Pleistocene glaciation upon oceanographic characteristics of the North Pacific Ocean and Bering Sea. *Deep Sea Research Part A. Oceanographic Research Papers* **30**: 851-869.
- Sarnthein M, Gebhardt H, Kiefer T, Kucera M, Cook M, Erlenkeuser H. 2004. Mid Holocene origin of the sea-surface salinity low in the subarctic North Pacific. *Quaternary Science Reviews* **23**: 2089-2099.
- Sarnthein M, Kiefer T, Grootes P.M, Elderfield H, Erlenkeuser H. 2006. Warmings in the far northwestern Pacific promoted pre-Clovis immigration to America during Heinrich event 1. *Geology* **34**: 141-144.
- Schmidt GA, Bigg GR, Rohling EJ. 1999. Global seawater oxygen-18 database. <http://data.giss.nasa.gov/o18data/>
- Schmidt M., Botz R, Stoffers P, Anders T, Bohrmann G. 1997. Oxygen isotopes in marine diatoms: A comparative study of analytical techniques and new results on the isotopic composition of recent marine diatoms. *Geochim. Cosmochim. Ac.* **61**: 2275-2280.
- Schmidt M, Botz R, Rickert D, Bohrmann G, Hall SR., Mann S. 2001. Oxygen isotope of marine diatoms and relations to opal-A maturation. *Geochim. Cosmochim. Ac.* **65**: 201-211.
- Shemesh A., Burckle L.H. and Hays J.D. 1994. Meltwater input to the Southern Ocean during the Last Glacial Maximum. *Science* **266**: 1542-1544.
- Shemesh A, Burckle LH, Hays JD. 1995. Late Pleistocene oxygen isotope records of biogenic silica from the Atlantic sector of the Southern Ocean. *Paleoceanography* **10**: 179-196.
- Spero HJ, Lea DW. 1993. Intraspecific stable isotope variability in the planktonic foraminifera *Globigerinoides sacculifer*: results from laboratory experiments. *Marine Micropaleontology* **22**: 221-234.
- Spero HJ, Lea DW. 1996. Experimental determination of stable isotope variability in *Globigerina bulloides*: implications for paleoceanographic reconstructions. *Marine Micropaleontology* **28**: 231-246.
- Spero HJ, Bijma J, Lea DW, Bemis B. 1997. Effect of seawater carbonate chemistry on planktonic foraminiferal carbon and oxygen isotope values. *Nature* **390**: 497-500.
- Sun Y, An Z. 2005. Late Pliocene-Pleistocene changes in mass accumulation rates of eolian deposits on the central Chinese Loess Plateau. *Journal of Geophysical Research*. Vol. **110**: D23101, doi:10.1029/2005JD006064.
- Swann GEA, Maslin MA, Leng MJ, Sloane HJ, Haug GH. 2006. Diatom  $\delta^{18}\text{O}$  evidence for the development of the modern halocline system in the subarctic North West Pacific at the onset of major Northern Hemisphere Glaciation. *Paleoceanography* **21**: PA1009, doi:10.1029/2005PA001147.
- Swann GEA, Leng MJ, Sloane HJ, Maslin MA, Onodera J. 2007. Diatom oxygen isotopes: evidence of a species effect in the sediment record. *Geochemistry, Geophysics, Geosystems* **8**: Q06012,

doi:10.1029/2006GC001535.

- Tabata S. 1975. The general circulation of the Pacific Ocean and a brief account of the oceanographic structure of the North Pacific Ocean. Part I, Circulation and volume transports. *Atmosphere* **13**: 134-168.
- Takahashi K. 1986. Seasonal fluxes of pelagic diatoms in the subarctic Pacific, 1982–1983. *Deep Sea Research Part A* **33**: 1225–1251.
- Takahashi K, Hisamichi K, Yanada M, Maita Y. 1996. Seasonal changes of marine phytoplankton productivity: a sediment trap study. *Kaiyo Mon.* **10**: 109–115. [In Japanese]
- Takeda S. 1998. Influence of iron availability on nutrient consumption ratio of diatoms in oceanic waters. *Nature* **393**: 774-777.
- Tsuda A, Takeda S, Saito H, Nishioka J, Nojiri Y, Kudo I, Kiyosawa H, Shiomoto A, Imai K, Ono T, Shimamoto A, Tsumune D, Yoshimura T, Aono T, Hinuma A, Kinugasa M, Suzuki K, Sohrin Y, Noiri Y, Tani H, Deguchi Y, Tsurushima N, Ogawa H, Fukami K, Kuma K, Saino T. 2003. A Mesoscale Iron Enrichment in the Western Subarctic Pacific Induces a Large Centric Diatom Bloom. *Science* **300**: 958-961.
- von Grafenstein U, Erlenkeuser H, Trumborn P. 1999. Oxygen and carbon isotopes in modern freshwater ostracod valves: assessing vital offsets and autecological effects of interest for palaeoclimate studies. *Palaeogeogr. Palaeocl.* **148**: 133–152.
- Wefer G, Berger WH. 1991. Isotope paleontology: growth and composition of extant calcareous species. *Mar. Geol.* **100**: 207-248.
- Xia J, and Engstrom DR, Ito E. 1997. Geochemistry of ostracode calcite: 1. an experimental determination of oxygen isotope fractionation. *Geochim. Cosmochim. Ac.* **61**: 377–382.
- Yamamoto M, Tanaka N, Tsunogai S. 2001. Okhotsk Sea intermediate water formation deduced from oxygen isotope systematics. *Journal of Geophysical Research* **106**: C12: 31,075-31,084.
- Yuan W, Zhang J. 2006. High correlations between Asian dust events and biological productivity in the western North Pacific. *Geophys. Res. Lett.* **33**: L07603, doi:10.1029/2005GL025174.

**Figure captions**

Figure 1: Location of ODP Site 882 (50°22'N, 167°36'E), North West Pacific Ocean, together with major ocean surface currents and the location of diatom monitoring station 50N (50.01°N, 165.01°E). Adapted from Figure 1 in Swann *et al.* (2007).

Figure 2: Typical light microscope images of diatoms analysed from ODP Site 882 at 4.7 ka BP, 72.4 ka BP and 115.7 ka BP ranging from 40-120 µm in diameter.

Figure 3: SEM images of diatoms analysed for  $\delta^{18}\text{O}$  at 4.7 ka BP, 75.9 ka BP, 96.8 ka BP and 115.7 ka BP.

Figure 4: A) Sample purity, percentage of diatom material relative to all other material in the cleaned samples. B) Relative diatom species biovolumes in purified samples analysed for  $\delta^{18}\text{O}_{\text{diatom}}$ . C) Comparison of  $\delta^{18}\text{O}_{\text{diatom}}$  measurements between the 38-75 µm fraction (up triangle) and the >100 µm fraction (down triangle) from 200 ka BP. Error bars for  $\delta^{18}\text{O}_{\text{diatom}}$  are within the size of the symbols. D)  $\delta^{18}\text{O}_{\text{diatom}}$  offsets between the two size fractions (>100 µm fraction minus 38-75 µm fraction). Dashed lines represent the RMSE of 0.56‰.

Figure 5:  $\delta^{18}\text{O}_{\text{diatom}}$  offsets (>100 µm fraction minus 38-75 µm fraction) mass balance corrected for contamination using a range of different theoretical  $\delta^{18}\text{O}_{\text{clay}}$  values. Amount of contamination in each sample is based on the diatom purity data (Fig. 4a).  $\delta^{18}\text{O}_{\text{diatom}}$  offset values on x-axis are the corrected offsets root squared in order to improve figure clarity. Dashed line represent the RMSE of 0.56‰.

**Table captions**

Table 1:  $\delta^{18}\text{O}_{\text{diatom}}$  data for the 38-75 µm and >100 µm size fractions. Offsets are difference in  $\delta^{18}\text{O}_{\text{diatom}}$  between the two size fractions (>100 µm fraction minus 38-75 µm fraction). Shaded values indicate offsets greater than the RMSE of 0.56‰.

Table 2: Modern day relative seasonal flux of *C. marginatus* and *C. radiatus* at station 50N (see Fig. 1) from December 1997 to May 2000. Data from Onodera *et al.*, (2005).

Table 3:  $\delta^{18}\text{O}_{\text{diatom}}$  offsets (>100 µm fraction minus 38-75 µm fraction) following corrections for diatom species seasonality and 1) SST seasonality; 2) SSS seasonality; 3) combined SST, SSS seasonality and depth habitats (see Section 4.2.1 for details). Shaded values indicate offsets greater than the RMSE of 0.56‰.

Table 1:

Age (ka) BP	$\delta^{18}\text{O}_{\text{diatom}}$ (‰)		Offset (‰)
	38-75 $\mu\text{m}$	>100 $\mu\text{m}$	
4.7	36.55	34.53	-2.02
9.1	40.14	39.82	-0.33
46.6	33.93	35.16	+1.23
51.3	36.86	39.76	+2.90
67.7	42.41	43.04	+0.63
72.4	41.55	42.63	+1.08
75.9	33.33	36.39	+3.07
80.3	31.82	29.32	-2.50
86.1	35.18	37.91	+2.74
92.2	39.34	42.09	+2.76
96.8	43.16	41.56	-1.60
99.3	41.90	39.82	-2.07
111.4	35.91	38.66	+2.75
115.7	39.53	41.20	+1.67
195.4	38.40	41.37	+2.97

Table 2:

Season	<i>C. marginatus</i> (%)	<i>C. radiatus</i> (%)
DJF	24.76	26.35
MAM	26.02	21.58
JJA	16.84	16.11
SON	32.38	35.96

Table 3:

Age (ka) BP	Original Offset (‰)	1) Offsets after SST correction	2) Offsets after SSS correction	3) Offsets after combined temperature, salinity and depth correction
4.7	-2.02	-2.04	-2.02	-2.17
9.1	-0.33	-0.38	-0.33	-0.58
46.6	+1.23	+1.20	+1.22	+0.82
51.3	+2.90	+2.86	+2.89	+2.60
67.7	+0.63	+0.55	+0.62	+0.41
72.4	+1.08	+1.02	+1.07	+0.71
75.9	+3.07	+3.04	+3.06	+2.75
80.3	-2.50	-2.53	-2.51	-2.98

86.1	+2.74	+2.71	+2.73	+2.44
92.2	+2.76	+2.74	+2.75	+2.11
96.8	-1.60	-1.61	-1.61	-2.24
99.3	-2.07	-2.08	-2.08	-2.59
111.4	+2.75	+2.73	+2.75	+2.38
115.7	+1.67	+1.66	+1.67	+1.27
195.4	+2.97	+2.97	+2.97	+2.45



Figure 1

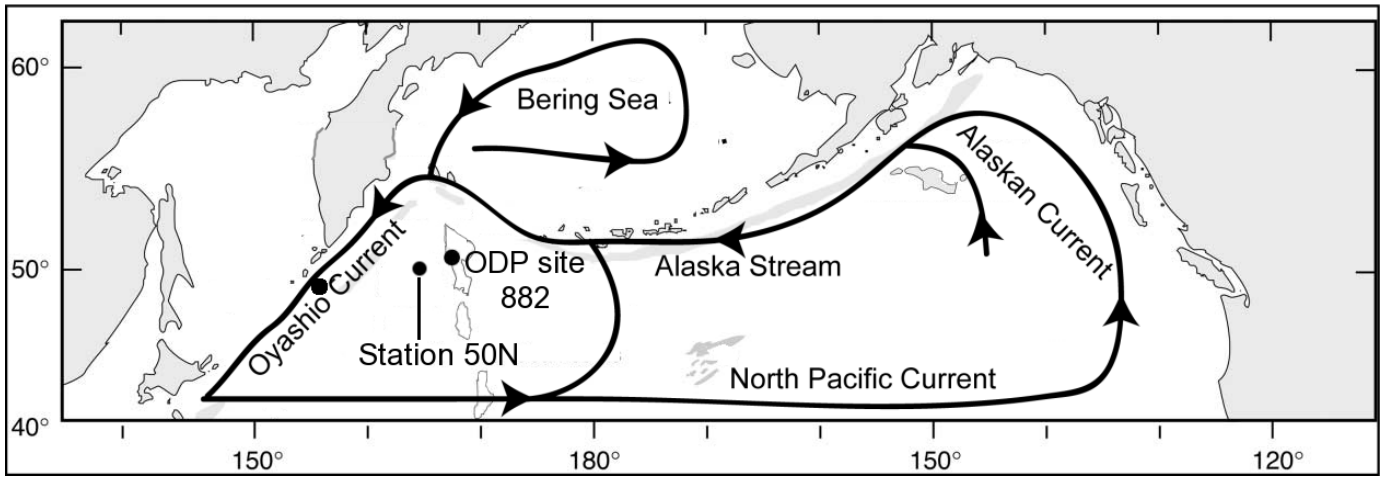




**Figure 2**

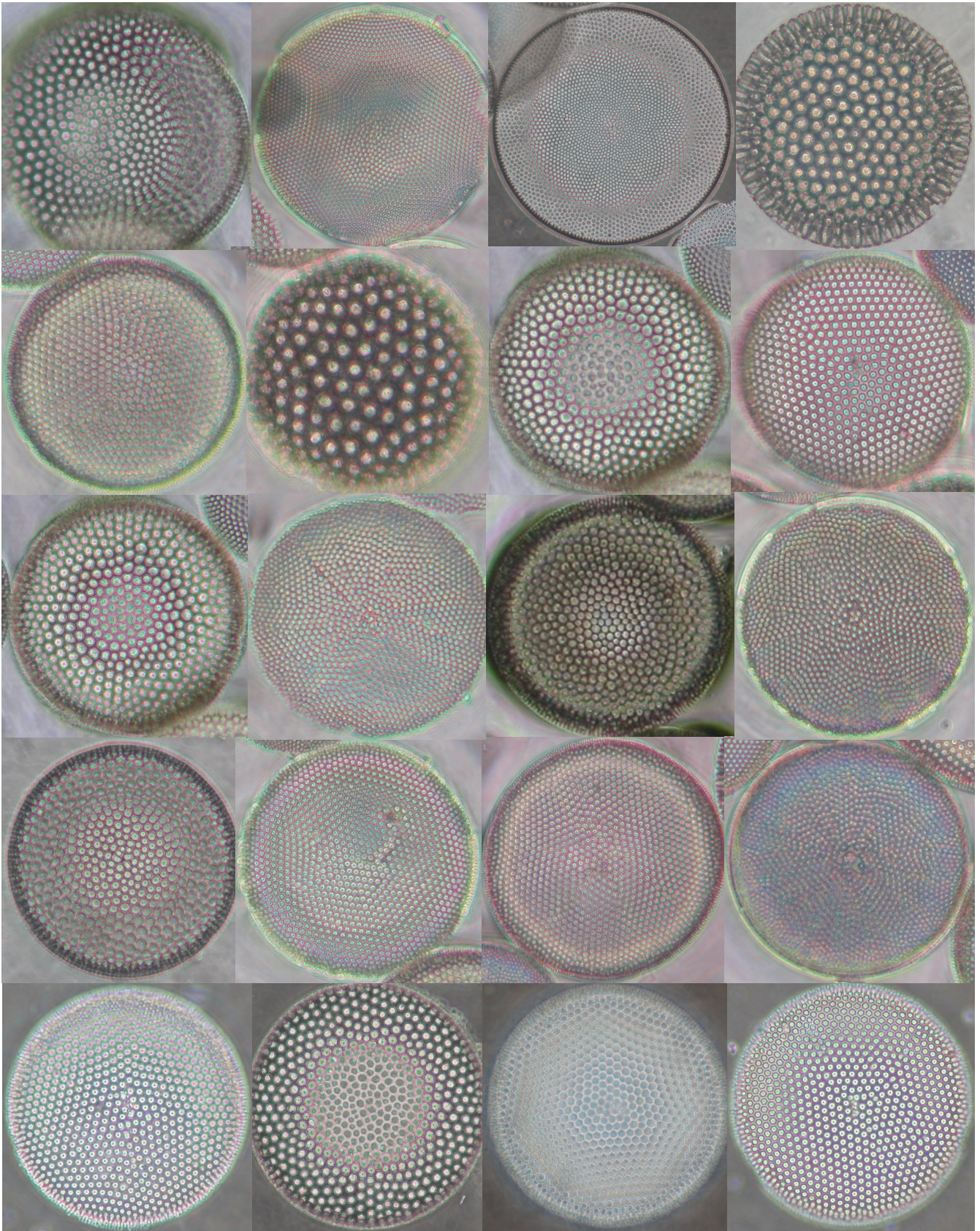




Figure 3

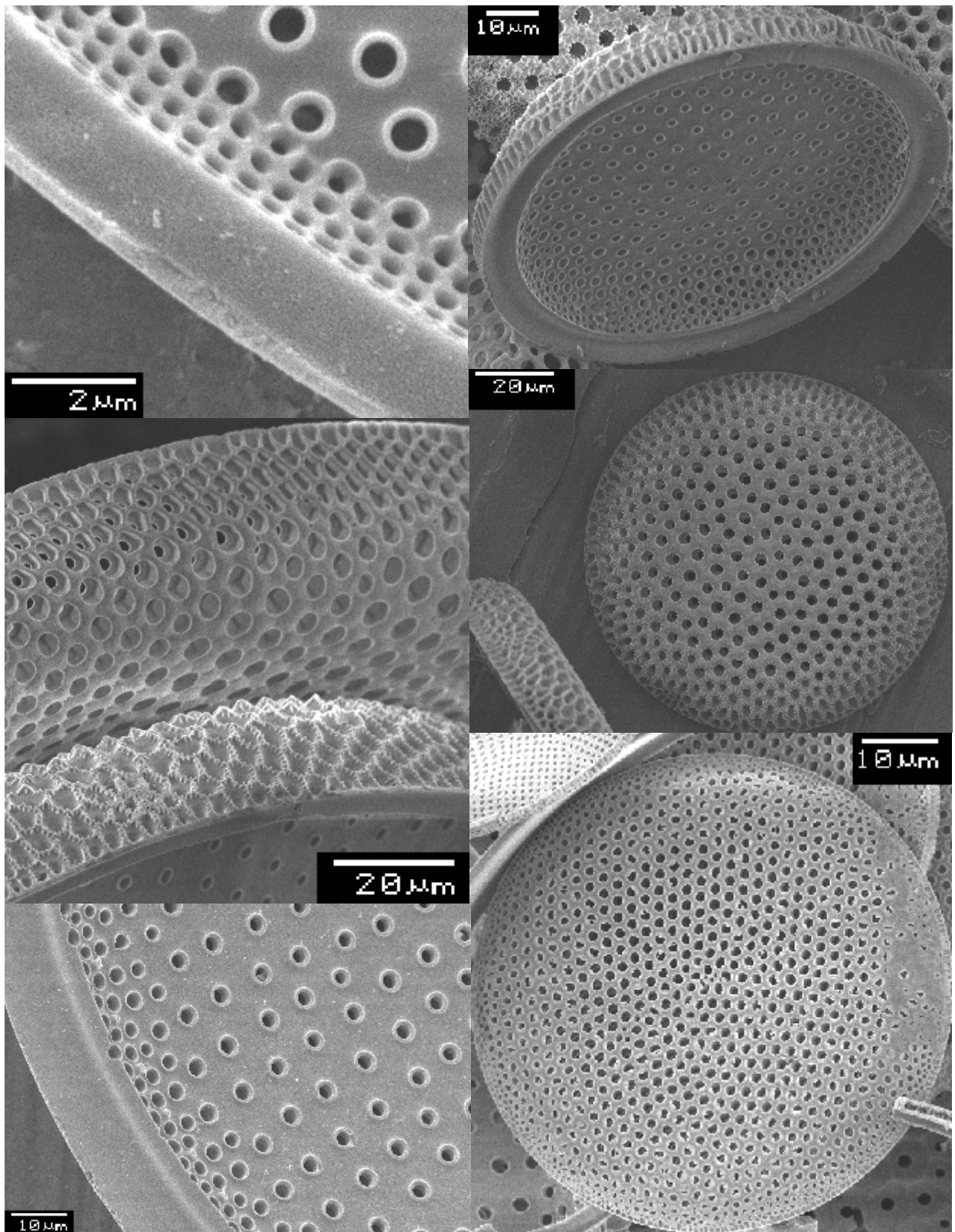


Figure 4

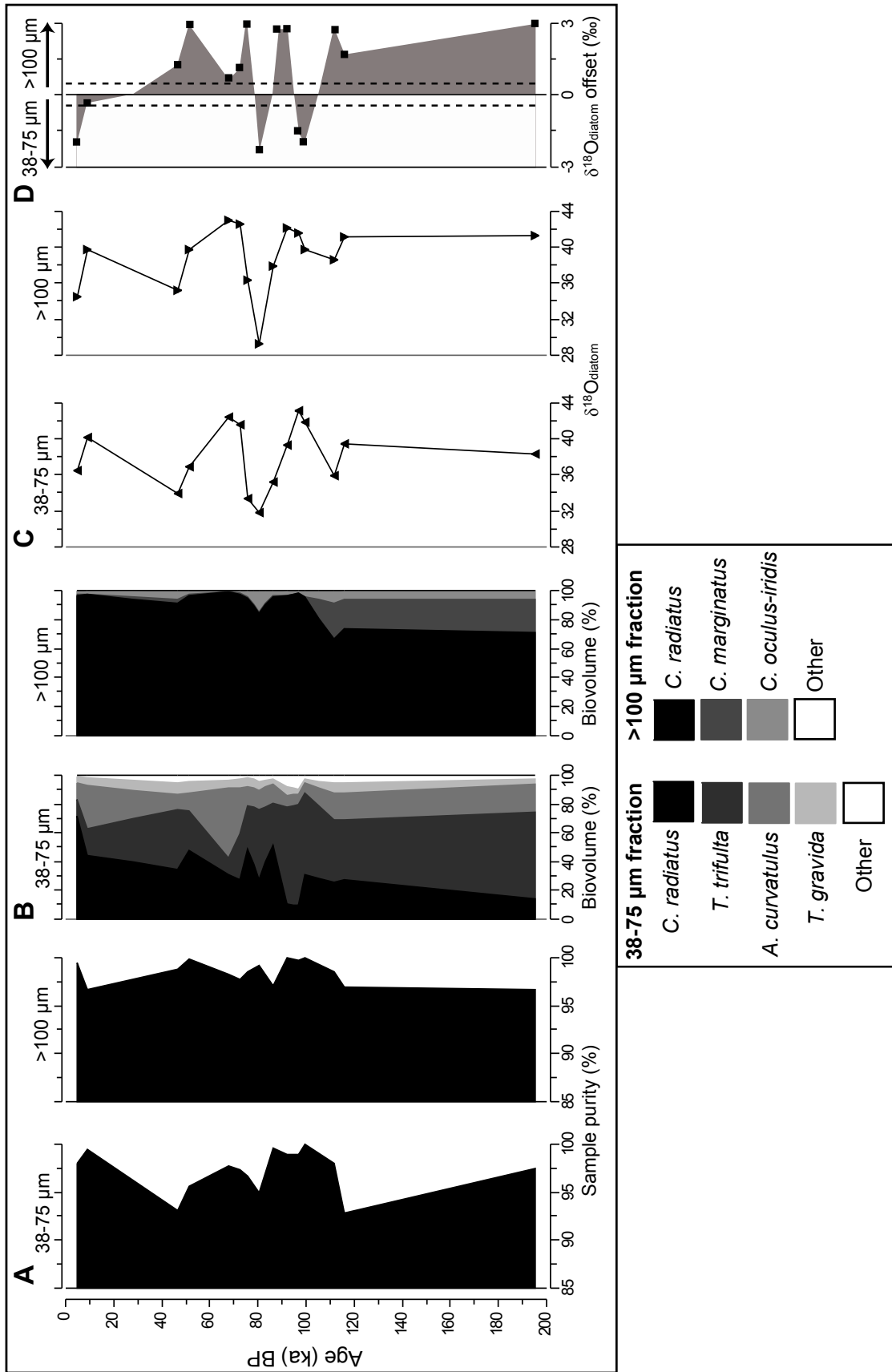


Figure 5

